This is the accepted manuscript made available via CHORUS. The article has been published as:

Phenomenological consequences of enhanced bulk viscosity near the QCD critical point

Akihiko Monnai, Swagato Mukherjee, and Yi Yin

Phys. Rev. C **95**, 034902 — Published 6 March 2017

DOI: 10.1103/PhysRevC.95.034902

Phenomenological Consequences of Enhanced Bulk Viscosity Near the QCD Critical Point

Akihiko Monnai,[1, 2] Swagato Mukherjee,[3] and Yi Yin[3]
[1]*RIKEN BNL Research Center, Brookhaven National Laboratory, Upton, NY 11973, USA*
[2]*Institut de Physique Théorique, CNRS URA 2306, CEA/Saclay, F-91191 Gif-sur-Yvette, France*
[3]*Department of Physics, Brookhaven National Laboratory, Upton, New York 11973-5000*

(Dated: February 17, 2017)

In the proximity of the QCD critical point the bulk viscosity of quark-gluon matter is expected to be proportional to nearly the third power of the critical correlation length, and become significantly enhanced. This work is the first attempt to study the phenomenological consequences of enhanced bulk viscosity near the QCD critical point. For this purpose, we implement the expected critical behavior of the bulk viscosity within a non-boost-invariant, longitudinally expanding $1+1$ dimensional causal relativistic hydrodynamical evolution at non-zero baryon density. We demonstrate that the critically-enhanced bulk viscosity induces a substantial non-equilibrium pressure, effectively softening the equation of state, and leads to sizable effects in the flow velocity and single particle distributions at the freeze-out. The observable effects that may arise due to the enhanced bulk viscosity in the vicinity of the QCD critical point can be used as complimentary information to facilitate searches for the QCD critical point.

I. INTRODUCTION

The structure of the QCD phase diagram has attracted much attention and triggered a plethora of theoretical and experimental studies (see Refs. [1–6] for reviews). Of high interest is the existence of a conjectured critical point [7–11] in the QCD phase diagram. This critical point is the end point of the first-order phase transition line that separates, in the chiral limit, a chirally symmetric quark-gluon plasma (QGP) phase from the hadron-matter phase of QCD. The existence of this critical point has been supported by many models of QCD thermodynamics. However, its precise location in the phase diagram and even its existence, is uncertain from the first-principle lattice simulations [4].

An entire experimental program, the Beam Energy Scan (BES) at the Relativistic Heavy-Ion Collider (RHIC) aims to search for the QCD critical point [5, 6]. A universal feature of a system near a critical point is the emergence of a critical mode, with growing and eventually divergent correlation length, ξ. Thus, physical quantities which are more sensitive to the growth of critical correlation length are expected to play crucial roles in experimental searches for the QCD critical point.

Well-known and more extensively studied examples are the non-Gaussian fluctuations of the critical mode which grow as high powers of ξ [12]. For example, while the variance grows as ξ^2, the skewness and the kurtosis are expected to grow more rapidly as $\xi^{4.5}$ and ξ^7, respectively. These enhanced near critical fluctuations are accessible through measurements of event-by-event fluctuations of particle multiplicities [11–14]. Expected growth of these fluctuation measures reflect the static properties of the underlying near critical background.

In the present work we pursue a complementary avenue — we focus on how the growth of ξ near the QCD critical point affects the bulk hydrodynamic evolution of the medium, and explore potential observables sensitive to such critical dynamics.

Hydrodynamical transport coefficients of a system near criticality scale with the correlation length with universal exponents, which are fixed by the dynamical universality class of the system. The dynamical universality class of the QCD critical point is argued to be that of model-H [15–17] according to the classification of Ref. [18]. For a system belonging to the dynamical universality class of model-H [1]

$$\eta \sim \xi^{\frac{1}{19}\epsilon}\,, \qquad \lambda \sim \xi\,, \qquad \text{and} \qquad D_B \sim 1/\xi\,, \tag{1}$$

where η, λ, and D_B denote the shear viscosity, thermal conductivity, and baryon diffusion constant, respectively. $\epsilon = 4-d$, where d is the spatial dimension. More importantly, near the criticality the bulk viscosity is expected to grow far more rapidly [19, 20] (see also Sec. II)

$$\zeta \sim \xi^3\,. \tag{2}$$

In view of the above behaviors of the transport coefficients, it is crucial to understand how the bulk hydrodynamical evolution of the matter created in heavy-ion collisions will be modified in the proximity of the QCD critical point, and what are the possible phenomenological consequences of such modification, if any. Previously, the hydrodynamical evolution near a critical point has been studied in a number of references [21–24] (see Ref. [25] for a recent review). While the critical behavior of the baryon diffusion constant was addressed in Ref. [26], studies incorporating critical behavior of bulk viscosity are sorely lacking.

---

[1] Throughout this work we use approximate rational values of critical exponents: $(\alpha,\beta,\gamma,\delta,\nu,\eta) = (0, 1/3, 4/3, 5, 2/3, 0)$. These approximate values are within few percents of their respective exact values.

This work is the first attempt to address this issue. We focus on the critical behavior of bulk viscosity as it exhibits the strongest dependence on the correlation length among the transport coefficients. As the first attempt, we incorporate the critical behavior of the bulk viscosity (*c.f.* Eq. (2)) within a non-boost-invariant, longitudinally expanding $1+1$ dimensional causal relativistic hydrodynamical equations (*i.e.* the Israel-Stewart theory [27]) at non-zero baryon density. Along the way, we also discuss the behavior of the bulk relaxation time, τ_Π, in the vicinity of the critical point. τ_Π is a transport coefficient in Israel-Stewart theory that controls the relaxation time of bulk viscous pressure towards its Navier-Stokes limit. We argue that near the QCD critical point $\tau_\Pi \sim \xi^3$. To best of our knowledge, the critical behavior of τ_Π has not been discussed before.

The rest of the paper is organized as follows. In Sec. II, we review the behavior of bulk viscosity and discuss the behavior of bulk relaxation time near the QCD critical point. We explain our set-up for hydrodynamic evolution in Sec. III. We present our results in Sec. IV and summarize in Sec. V.

II. BULK VISCOSITY AND RELAXATION TIME NEAR QCD CRITICAL POINT

We consider the following second order viscous hydrodynamic equations with finite baryon density

$$\nabla_\mu T^{\mu\nu} = 0\,, \tag{3a}$$

$$\nabla_\mu J^\mu_B = 0\,, \tag{3b}$$

$$u^\mu \partial_\mu \Pi = -\frac{1}{\tau_\Pi}\left[\,\zeta \partial_\mu u^\mu + \Pi\,\right], \tag{3c}$$

where ∇ denotes the covariant derivative in Bjorken coordinates. The stress-energy tensor is decomposed as $T^{\mu\nu} = \epsilon u^\mu u^\nu + (p+\Pi)\,\Delta^{\mu\nu} + \pi^{\mu\nu}$, where ϵ, p, u^μ are the equilibrium energy density, the equilibrium pressure and the fluid velocity, respectively. The bulk viscous pressure Π measures the deviation of the pressure from its equilibrium value. $\Delta^{\mu\nu} = g^{\mu\nu} + u^\mu u^\nu$ projects onto the spatial components in the local rest frame, and $\pi^{\mu\nu}$ is the shear-viscous stress tensor. Our sign convention for the metric is chosen to be $g^{\mu\nu} = \mathrm{diag}(-1,+1,+1,+1)$. Since the bulk viscosity exhibits the strongest dependence on ξ, we will concentrate solely on the effects of the bulk viscosity. More specifically, in Eq. (3) we only keep terms involving the bulk viscosity, ζ, and the bulk relaxation time, τ_Π, completely omitting terms involving the shear viscous tensor, $\pi^{\mu\nu}$, as well as the baryon density diffusion. More specifically, we use the baryon current $J^\mu_B = n_B u^\mu$, n_B being the baryon density, and do not include terms in the baryon current which are proportional to the baryon diffusion.

Now, we discuss the behaviors of ζ and τ_Π near the QCD critical point. The behavior of ζ can be determined by noting that the dynamical universal behavior of the QCD critical point is the same as for the liquid-gas phase transition [15, 16], *i.e.* that of model-H [18]. Onuki has performed a detailed study of the behavior of the bulk viscosity near the critical point of a liquid-gas system [20], and it can be directly adapted for the case of QCD critical point: $\zeta \sim \xi^{z-\alpha/\nu}$. Here, α and ν are standard equilibrium critical exponents, and z is the dynamical critical exponent. At the mean-field level $\alpha = 0$, and $z = 3$ for the model-H [20], giving: $\zeta \sim \xi^3$.

An intuitive explanation of the behavior of bulk viscosity in the vicinity of the critical point goes as follows [19] — bulk viscosity controls the relaxation time of the pressure towards its equilibrium value after a rapidly applied small compression or expansion. Near a critical point, the pressure will remain out of equilibrium until the slow critical mode relaxes back to its equilibrium value, and, thus, $\zeta \propto \tau_\sigma$, where τ_σ is the relaxation time for the critical mode. Due to the critical slowing down τ_σ provides the longest time scale, and grows as $\tau_\sigma \sim \xi^z$ [18]. Hence, in the proximity of a critical point the bulk viscosity is expected to be enhanced as $\zeta \sim \tau_\sigma \sim \xi^z$.

The above discussion also sheds light on the behavior of τ_Π near a critical point. Imagine a homogeneous equilibrated system, described by the equilibrium values of ϵ, p, and with $\Pi = 0$ and $u^\mu = (1,0,0,0)$. Now, consider a small homogeneous, but time-dependent perturbation of the bulk pressure, $\delta\Pi$. Since such a perturbation has no spatial dependence, $\delta\Pi$ does not change the energy-momentum conservation equation Eq. (3a). Consequently, $\partial_\mu u^\mu = 0$, and Eq. (3c) becomes $\partial_t \delta\Pi = -\delta\Pi/\tau_\Pi$, implying that the characteristic damping-time of the off-equilibrium pressure, Π, is given by τ_Π. Near a critical point this time scale should be governed by the relaxation time of the slowest mode, *i.e.* that of the critical mode, given by $\tau_\sigma \sim \xi^z$. Thus, near a critical point it is natural to expect: $\tau_\Pi \sim \tau_\sigma \sim \xi^z$.

The above argument can be further supplemented and strengthened by invoking causality of the Israel-Stewart theory. For the linearized Israel-Stewart theory, neglecting the contribution of shear viscosity, the dispersion relation of the sound mode is given by [28]

$$\lim_{k\to\infty} \frac{d\omega_{\text{sound}}(k)}{dk} = \sqrt{c_s^2 + \frac{\zeta}{\tau_\Pi\,(\epsilon+p)}}\,, \tag{4}$$

where c_s denotes the speed of sound. To maintain causality the sound speed cannot exceed the speed of light, *i.e.* the right hand side of the above equation must remain less than 1. In other words, to ensure causality $\zeta/\tau_\Pi\,(\epsilon+p)$ must remain finite, and cannot grow with the diverging correlation length near a critical point. Since near a critical point $(\epsilon+p)$ remains non-zero but the bulk viscosity diverges as $\zeta \sim \xi^z$, causality dictates that the bulk relaxation time also must grow at least as rapidly as $\tau_\Pi \sim \xi^z$.

Thus, near a critical point the bulk relaxation time is expected to diverge as

$$\tau_\Pi \sim \xi^z \,. \tag{5}$$

While Eq. (5) is a natural consequence of slow relaxation of the critical modes, to best of our knowledge, the critical behavior of τ_Π has not been discussed in literature before.

To summarize, ζ and τ_Π determines the relaxation of pressure towards its equilibrium value in long time limit, and, near a critical point, this relaxation process is governed by the relaxation of the slowest critical modes. In particular, for the QCD critical point belonging to the dynamical universality class of model-H, we, therefore, have

$$\zeta \sim \tau_\Pi \sim \tau_\sigma \sim \xi^3 \,. \tag{6}$$

With the critical behaviors ζ and τ_Π at hand, we are now ready to study their influences on hydrodynamic evolution near the QCD critical point.

III. SET-UP FOR HYDRODYNAMIC EVOLUTION

In this exploratory study we consider $1+1$ dimensional Israel-Stewart hydrodynamics with longitudinal expansion along the z-direction [29]. The temperature, baryon density and fluid velocity only depend on the proper time $\tau = \sqrt{t^2 - z^2}$ and spatial rapidity $\eta = \arctan(z/t)$, and the fluid velocity is given by $u^\mu = (u^\tau, u^\eta, 0, 0)$.

We numerically solve the $1+1$ dimensional non-boost-invariant viscous hydrodynamic equations, Eqs. (3). The spatial rapidity dependence of the initial energy and baryon number densities are obtained by extrapolating color glass models [30–33] to the fixed beam energy $\sqrt{s} = 17$ GeV, see Fig. 1. The normalizations and parameters in those models are tuned to roughly imitate the rapidity distributions of the charged hadrons and the net baryon number of the most central Pb-Pb collisions at SPS near mid-rapidity at the corresponding beam energy. The initial state model used in this study might not be completely realistic for heavy-ion collisions at the lower energy. However, they suffice for this illustrative study. Since at this beam energy the two incoming nuclei take longer to pass through each other, we start the hydrodynamic evolution at $\tau_{\rm th} = 1.5$ fm/c. We further assume $u^\eta(\tau_{\rm th}) = 0$ and $\Pi(\tau_{\rm th}) = 0$.

Hydrodynamical equations are closed by providing an equation-of-state (EoS), $p(\mu_B, T)$, $\epsilon(\mu_B, T)$ and $n_B(\mu_B, T)$. The EoS is constructed out of the second- and fourth-order net-baryon number fluctuations computed using lattice QCD [34–36], and by matching onto that obtained from a hadron resonance gas model at low temperatures [37, 38]. As our sole focus is on the effects of the critical enhancement of bulk viscosity, for simplicity, we do not include any critical behavior in the EoS itself.

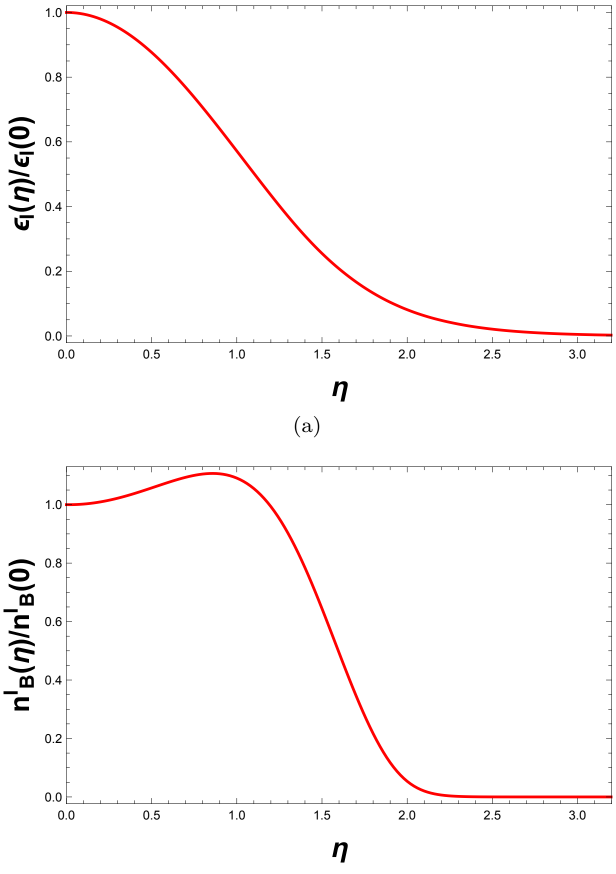

(a)

(b)

FIG. 1. (Color online) Dependence of initial energy density, $\epsilon_I(\eta)$ (a), and initial baryon number density, $n_B^I(\eta)$ (b), normalized by their corresponding values at $\eta = 0$, on the spatial rapidity, η.

For further quantification this critical enhancement, we consider two cases with the same initial condition. In the first case, denoted by "no-CP", we solve (3) by assuming that the QCD critical regime is far away from the evolution trajectories in the μ_B-T plane. In the second case, denoted by "CP", the location and width of the critical region are chosen to make some evolution trajectories pass through the critical regime.

To study the hydrodynamic evolution near the critical point we implement critical behaviors of ζ and τ_σ within a chosen critical region. First, we define the QCD critical region as the area enclosed by equal correlation length contour $\xi(\mu_B, T) = \xi_0$, where ξ_0 is the value of the correlation length at the edge of the critical regime (c.f. Fig. 2). Within this critical region we use

$$\zeta = \zeta_0 \left(\frac{\xi}{\xi_0}\right)^3 , \qquad \text{and} \qquad \tau_\Pi = \tau_\Pi^0 \left(\frac{\xi}{\xi_0}\right)^3 , \tag{7}$$

in accordance with Eq. (6). ζ_0 and τ_Π^0 are the bulk viscosity and bulk relaxation time outside the critical region, respectively. Our choice for the (T, μ_B)-dependence of ζ_0 and τ_Π^0 are motivated by the holographic model based results of Refs. [39, 40]

$$\zeta_0 = 2\left(\frac{1}{3} - c_s^2\right)\frac{e+p}{4\pi T}\,, \tag{8a}$$

$$\tau_\Pi^0 = C_\Pi \frac{18 - (9\ln 3 - \sqrt{3}\pi)}{24\pi T}\,. \tag{8b}$$

To study the effects of relaxation time in more detail we consider hydrodynamic evolutions with different choices of C_Π.

Next, we model how ξ varies over the μ_B-T plane, *i.e.* $\xi(\mu_B, T)$. Near the Ising critical point the dependence of $\xi(r,h)$ on the Ising variables, the reduced temperature r and the re-scaled magnetic field h, is universal. For convenience of the readers the details on $\xi(r,h)$ are provided in Appendix. A. However, the mapping of the Ising variables (r,h) onto the thermodynamic variables (μ_B, T) is not universal. For simplicity, we will follow the widely-used prescription (see for example [22, 41, 42])

$$\frac{T - T_c}{\Delta T} = \frac{h}{\Delta h}\,, \qquad \frac{\mu_B - \mu_B^c}{\Delta\mu_B} = -\frac{r}{\Delta r}\,. \tag{9}$$

Here, (μ_B^c, T_c) is the location of the QCD critical point, and $(\Delta\mu_B, \Delta T)$ is the width of the critical region in the μ_B-T plane. The corresponding width of the critical region in term of the Ising variables $(\Delta r, \Delta h)$ is defined to be

$$\xi(r = \Delta r, h = 0) = \xi(r = 0, h = \Delta h) = \xi_0\,. \tag{10}$$

Specifically, the width of the QCD critical region is chosen to be $(\Delta\mu_B, \Delta T) = (0.1, 0.02)$ GeV, surrounding the critical point located at $(\mu_B^c, T_c) = (0.22, 0.16)$ GeV. For numerical convenience, we set a upper limit for ξ, *i.e.* $\xi_{\max} = 10\xi_0$. One might wonder that our choice of μ_B^c, T_c are unreasonable based upon our current knowledge of the QCD phase diagram. However, for our illustrative purpose, this choice is a simple convenient way to make comparisons between evaluations with and without the presence of a critical point, keeping other inputs (initial condition, EoS *etc.*) unchanged. The boundary of the critical region in the μ_B-T plane is illustrated in Fig. 2.

Finally, we end the hydrodynamic evolution and compute particle distributions using the Cooper-Frye formalism on a (thermal) freeze-out surface characterized by a constant energy density $\epsilon_f = 0.25$ GeV/fm^3. This corresponds to freeze-out temperature $T_f \sim 0.15$ GeV at vanishing chemical potential. The freeze-out curve in the μ_B-T plane is also shown in Fig. 2.

The bulk viscosity modifies the one-particle phase-space distribution in the Cooper-Frye formula. This distortion of the distribution δf is determined using the Grad's moment expansion and the self-consistency conditions that off-equilibrium components of the energy-momentum tensors and net baryon number currents in kinetic theory and hydrodynamics match respectively [27]. See Ref. [43] for the specific form.

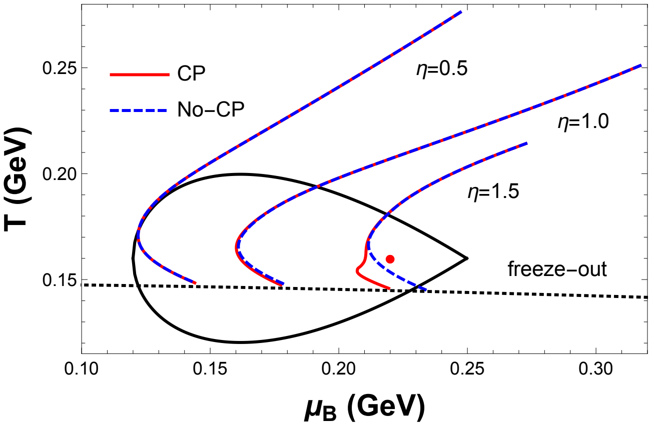

FIG. 2. (Color online) Hydrodynamic evolution trajectories in the μ_B-T plane for different spatial rapidity, η, as well as with and without the presence of a critical point. Black solid curve plots the equal-ξ contour, *i.e.* the critical region, with the red dot illustrating the position of the critical point, see text.

IV. RESULTS

A. Trajectories in the μ_B-T plane

The trajectories in the μ_B-T plane resulted from our hydrodynamic evolution, with τ_Π corresponding to $C_\Pi = 1$, are shown in Fig. 2. The trajectories for the CP and no-CP scenarios are nearly identical except for those corresponding to $\eta = 1.5$, *i.e.* the one closest to the critical point. The large value of ζ in the vicinity of the critical point produces more entropy, and 'pushes' the trajectory towards smaller values of μ_B. Consequently, trajectories passing the crossover side of the critical regime move further away from the critical point.

B. Bulk viscous pressure and flow

We now turn to bulk viscous pressure by focusing on the evolution of Π along the trajectory corresponding to $\eta = 1.5$ for the CP scenario. First, in Fig. 3(a) we show the critical enhancement of the relevant dimensionless quantity ζ/s along this trajectory, s being the entropy density. This enhanced bulk viscosity leads to a dramatic reduction of the bulk viscous pressure, as shown in Fig. 3(b). For reference, in the same figure we also show the corresponding Navier-Stokes value (black dotted line) and the no-CP scenario (black dashed line). The growth of Naiver-Stokes value, $\zeta\,(\partial_\mu u^\mu)$, in the critical regime is in accordance with the growth of ζ. While for no-CP $|\Pi|$ is an order of magnitude smaller than the equilibrium pressure, for CP $|\Pi|$ can become comparable to the equilibrium pressure within the critical regime.

To clarify the role of τ_Π in the critical regime we solve Eq. (3) for several values of τ_Π, corresponding to different choices of C_Π. These results are shown in Fig. 3(b).

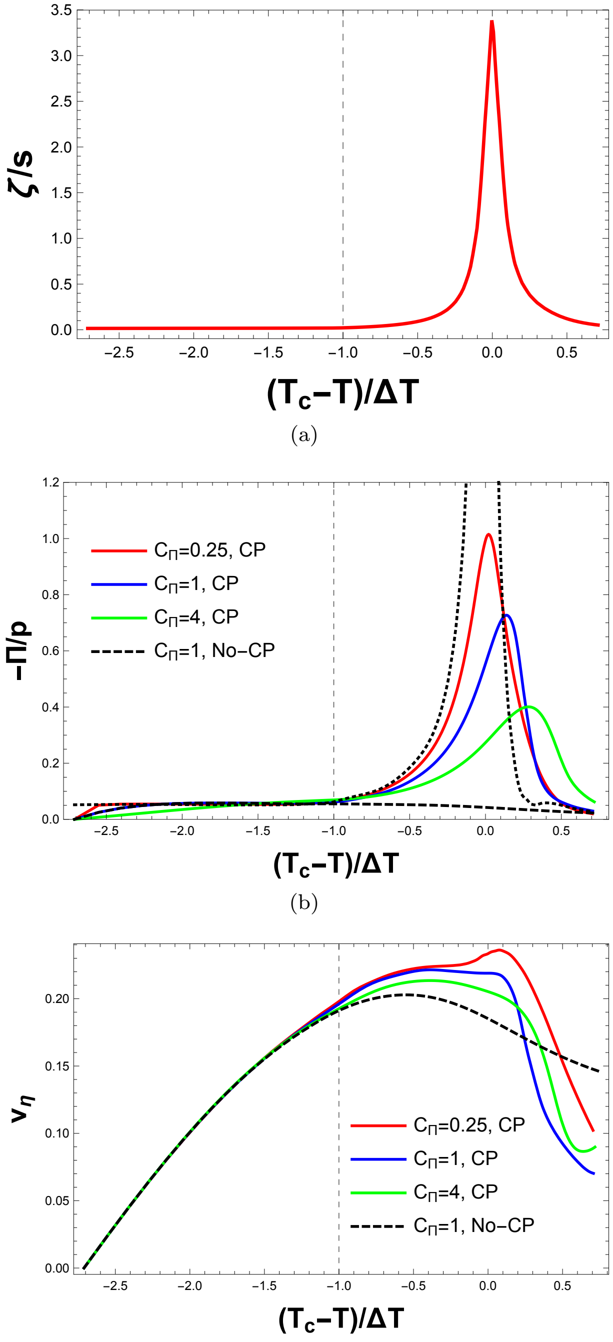

(a)

(b)

(c)

FIG. 3. (Color online) The ratios of bulk viscosity to entropy density ζ/s (a), bulk viscous pressure to equilibrium pressure Π/p (b), and the fluid velocity $v_\eta = u^\eta/u^\tau$ (c) along the hydrodynamic evolution trajectory corresponding to spatial rapidity $\eta = 1.5$ and in presence of a critical point. Results for evolution with several values of the bulk relaxation time τ_Π corresponding to $C_\Pi = 0.25, 1$ and 4 (see Eq. 8b) are shown by red, blue and green curves, respectively. The Navier-Stokes limit along the same trajectory in the presence of the critical point also is shown by the black dotted curve. The black dashed curves show results in absence of a critical point and with $C_\pi = 1$.

As expected, a larger bulk relaxation time not only reduces the maximal value $|\Pi|$ but also delays the growth. Note that, such delayed growths make $|\Pi|$ substantially larger than its Navier-Stokes limits at later times. Similar observations regarding finite-time effects were made in previous studies of on critical fluctuations [41, 42]; for off-equilibrium critical universal behavior induced by finite-time effects, see Ref. [44].

It is easy to infer the effective pressure, $p_{\rm eff} = p + \Pi$, from the Π/p in Fig 3(b). While for no-CP $p_{\rm eff}$ is not much different from the equilibrium pressure, in the presence of a critical point $p_{\rm eff}$ can be significantly suppressed and become nearly vanishing depending on the largeness of τ_Π.

In Fig. 3(c) we show the flow velocity, $v_\eta = u^\eta/u^\tau$ along the same trajectory for different values of τ_Π. Since the acceleration rate of flow rapidity is proportional to the spatial gradients of $p_{\rm eff}$, for CP we observe significantly large v_η due the smaller $p_{\rm eff}$ at the forward-rapidity.

C. Rapidity distributions of hadrons

We now present couple observables accessible in the heavy-ion collision experiments. We choose charged particle and net-baryon number multiplicities, $N_{\rm ch}$ and $N_{\rm B}$ respectively, per unit momentum rapidity Y. The $dN_{\rm ch}/dY$ and $dN_{\rm B}/dY$ are obtained at the freeze-out, carried out following the procedure described before.

Our results for $dN_{\rm ch}/dY$ are shown in Fig 4. In addition, we have also found that the influence of the non-critical bulk viscosity, *i.e.* in the no-CP scenario, on $dN_{\rm ch}/dY$ without δf is a mere few percent. For no-CP $dN_{\rm ch}/dY$ decreases monotonically with increasing Y, similar to the $\epsilon_I(\eta)$ in Fig. 1(a). In contrast, for the CP case $dN_{\rm ch}/dY$ becomes non-monotonic in Y, showing a large increase around $Y = 2$. These charged particles likely come from trajectories which are closer to the critical point, see Fig. 2. Here one should note that there is correlation between η and Y even after thermal smearing. The enhanced particle production might be understood intuitively by noting that growth of bulk viscosity (2) in the vicinity of the QCD critical point induces an increase in entropy thus is accompanied by an increase in multiplicity. The effects of enhanced entropy production due to bulk viscosity near the critical point has also been discussed in Ref. [45]. Additionally, the spatial gradient of $p_{\rm eff}$ is steepened by the large bulk viscosity, accelerating the flow as indicated in Fig. 3(c). The entropy density is then carried from mid-rapidity to forward rapidity because the entropy current is associated with the flow. This explains slight reduction of multiplicity at mid-rapidity in Fig. 4(a). As shown explicitly in Fig. 4(b), the presence of a critical point can enhance $dN_{\rm ch}/dY$ in the forward-rapidity by as much as 30%.

In Fig. 5 we present results for $dN_{\rm B}/dY$. The influence of a critical point is similar to that in the case of charged

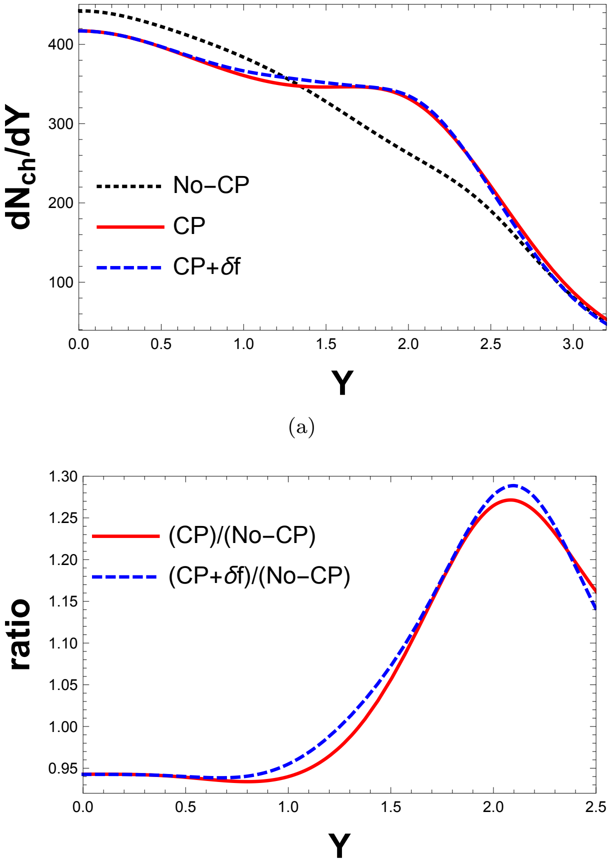

(a)

(b)

FIG. 4. (Color online) (a) Charge particle multiplicity per unit momentum rapidity, $dN_{\rm ch}/dY$, as a function of Y. The dashed black, solid red and dashed blue curves, respectively, correspond to results for hydrodynamical evolution with (CP) without (no-CP) a critical point, as well as including the non-equilibrium δf contribution to the freeze-out (CP+δf). (b) The relative change of $dN_{\rm ch}/dY$ with and without a critical point.

particles. Since the entropy production in presence of large viscosity will not change the net-baryon number, the enhancement in $dN_{\rm B}/dY$ at the forward-rapidity is the effect of enhanced convection caused by the larger spatial gradient in $p_{\rm eff}$. The relative enhancement around $Y = 2$ in Fig. 5(b) is, thus, smaller than that for the $dN_{\rm ch}/dY$ in Fig. 4(b).

V. SUMMARY AND DISCUSSIONS

This work is the first exploratory attempt to study the consequences of the anticipated enhancement of bulk viscosity near the QCD critical point. We incorporated the expected critical behaviors of the bulk viscosity and relaxation time in Eq. (6) within a non-boost-invariant, longitudinally expanding $1 + 1$ dimensional causal relativistic hydrodynamical evolution at non-zero baryon density. To clarify the influence of the critically-enhanced bulk viscosity we compared results from hydrodynamic evolution with and without the presence of a critical point, but using the same initial conditions and the EoS. As shown in Figs. 4(b) and 5(b), we found that the critically-enhanced bulk viscosity led to a sizable increase of $dN_{\rm ch}/dY$ and $dN_{\rm B}/dY$ at forward-rapidity; suggesting that particle spectra may contain discernible information regarding the presence of a critical point in the QCD phase diagram. Also, we have demonstrated that presence of a critical point will lead to a rapid growth of the bulk viscous pressure, which in turn will soften the effective pressure. In future, it will be interesting to explore whether such softening of the effective pressure can lead to the observed non-monotonicity, as function of $\sqrt{s}$, in the slope of the directed flow of net-protons [46] or that in the re-scaled triangular flow [47], as these features are sometime speculated to be related to the softening of

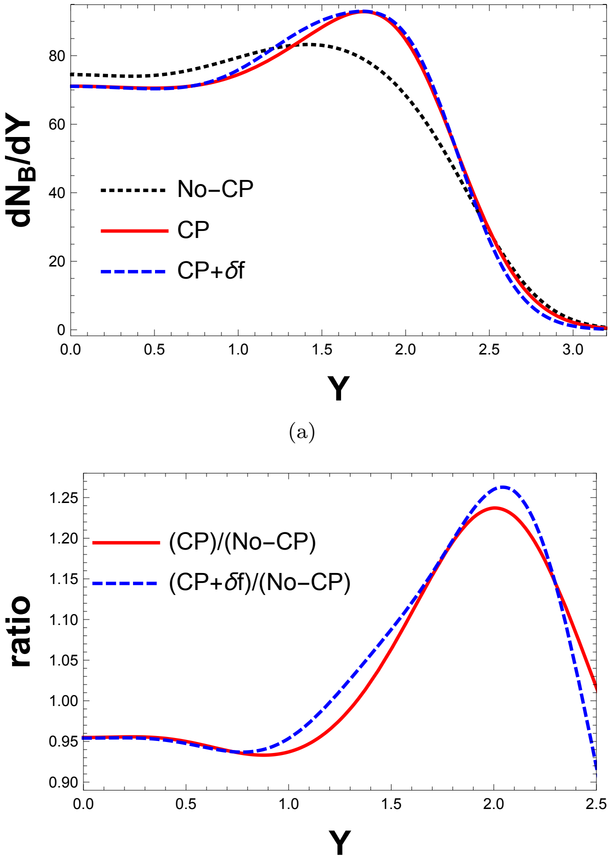

(a)

(b)

FIG. 5. (Color online) (a) Net-baryon multiplicity per unit momentum rapidity, $dN_{\rm B}/dY$, as a function of Y. The dashed black, solid red and dashed blue curves, respectively, correspond to results for hydrodynamical evolution with (CP) without (no-CP) a critical point, as well as including the non-equilibrium δf contribution to the freeze-out (CP+δf). (b) The relative change of $dN_{\rm B}/dY$ with and without a critical point.

the pressure. Of course, such questions must be carefully addressed using state-of-the-art hydrodynamic evolutions, and goes much beyond the scope of our present exploratory illustrative study involving only longitudinal expansion, simplified initial conditions and non-critical EoS. Use of state-of-the-art hydrodynamic evolution also will enable access to transverse momentum spectra and azimuthal momentum anisotropy, which were shown to be more sensitive to the bulk viscosity [48].

We close with a short discussion on the applicability of the hydrodynamic with a large bulk viscosity. Obviously, when $p_{\rm eff} < 0$ hydrodynamical evolution becomes mechanically unstable against cavitation, as has been discussed in a number of references [49] previously. Indeed, if Π is close to its corresponding Navier-Stokes value, the cavitation seems unavoidable for trajectories near the critical point. However, as we have already discussed, the presence of τ_Π limits the growth of Π. Consequently, in our current case, cavitation may only happen for very small values of τ_Π corresponding to $C_\Pi < 0.25$, see for example the solid red curve in Fig. 3(b). Furthermore, as pointed out in Ref. [48], when the viscosity is too large then one also needs to worry about the applicability of the Israel-Stewart formalism, namely the bulk viscous corrections to the energy-momentum tensor must be much smaller compared to the ideal fluid terms, $|\Pi|/(\epsilon + p) \ll 1$. When $|\Pi| \sim p$, one has $|\Pi|/(\epsilon + p) \sim 1/(1 + c_s^{-2})$. For $\mu_B = 0$ and around the transition temperature T_c, the value of c_s^2 is about 0.15 [34], giving $|\Pi|/(\epsilon + p) \sim 0.1$. Closer to the critical point and around the cross-over line the equation of state is expected to become even softer, leading to an even smaller value of c_s^2, and thus extending the the range of applicability of Israel-Stewart formalism.

One can also see in Figs. 4 and 5 that the contributions of the bulk viscous corrections δf to the particle spectra are small even when $|\Pi| \sim p$.

ACKNOWLEDGMENTS

We would like to thank G. Denicol, U. Heinz, R. Pisarski, L. McLerran, K. Rajagopal, P. Sorensen, and M. Stephanov for very valuable discussions and M. Nahrgang, T. Schäfer, and B. Schenke for commenting on the manuscript. AM was supported in part by RIKEN Special Postdoctoral Researcher program and JSPS Postdoctoral Fellowship for Research Abroad. This material is based upon work supported by the U.S. Department of Energy, Office of Science, Office of Nuclear Physics, under Contract No. DE-SC0012704, and within the framework of the Beam Energy Scan Theory (BEST) Topical Collaboration.

[1] M. A. Stephanov, Prog. Theor. Phys. Suppl. **153**, 139 (2004).
[2] M. Stephanov, PoS **LAT2006**, 024 (2006).
[3] K. Fukushima and T. Hatsuda, Rept. Prog. Phys. **74**, 014001 (2011).
[4] H.-T. Ding, F. Karsch, and S. Mukherjee, Int. J. Mod. Phys. **E24**, 1530007 (2015).
[5] "Studying the phase diagram of qcd matter at rhic," (2014), `https://drupal.star.bnl.gov/STAR/files/BES_WPII_ver6.9_Cover.pdf`.
[6] U. Heinz, P. Sorensen, A. Deshpande, C. Gagliardi, F. Karsch, *et al.*, arXiv:1501.06477 [nucl-th].
[7] M. Asakawa and K. Yazaki, Nucl. Phys. **A504**, 668 (1989).
[8] A. Barducci, R. Casalbuoni, S. De Curtis, R. Gatto, and G. Pettini, Phys. Lett. **B231**, 463 (1989).
[9] A. M. Halasz, A. Jackson, R. Shrock, M. A. Stephanov, and J. Verbaarschot, Phys. Rev. **D58**, 096007 (1998).
[10] J. Berges and K. Rajagopal, Nucl. Phys. **B538**, 215 (1999).
[11] M. A. Stephanov, K. Rajagopal, and E. V. Shuryak, Phys. Rev. Lett. **81**, 4816 (1998).
[12] M. Stephanov, Phys. Rev. Lett. **102**, 032301 (2009).
[13] Y. Hatta and M. Stephanov, Phys. Rev. Lett. **91**, 102003 (2003).
[14] C. Athanasiou, K. Rajagopal, and M. Stephanov, Phys. Rev. **D82**, 074008 (2010).
[15] D. Son and M. Stephanov, Phys. Rev. **D70**, 056001 (2004).
[16] H. Fujii, Phys. Rev. **D67**, 094018 (2003); H. Fujii and M. Ohtani, Prog. Theor. Phys. Suppl. **153**, 157 (2004).
[17] H. Fujii and M. Ohtani, Phys. Rev. **D70**, 014016 (2004).
[18] P. C. Hohenberg and B. I. Halperin, Rev. Mod. Phys. **49**, 435 (1977).
[19] G. D. Moore and O. Saremi, JHEP **09**, 015 (2008).
[20] A. Onuki, Phys. Rev. E **55**, 403 (1997).
[21] K. Paech, H. Stoecker, and A. Dumitru, Phys. Rev. **C68**, 044907 (2003).
[22] C. Nonaka and M. Asakawa, Phys. Rev. **C71**, 044904 (2005).
[23] K. Paech and A. Dumitru, Phys. Lett. **B623**, 200 (2005).
[24] C. Herold, M. Nahrgang, I. Mishustin, and M. Bleicher, Phys. Rev. **C87**, 014907 (2013).
[25] M. Nahrgang, (2016), arXiv:1601.07437 [nucl-th].
[26] J. I. Kapusta and J. M. Torres-Rincon, Phys. Rev. **C86**, 054911 (2012).
[27] W. Israel and J. M. Stewart, Annals Phys. **118**, 341 (1979).
[28] P. Romatschke, Int. J. Mod. Phys. **E19**, 1 (2010).
[29] A. Monnai, Phys. Rev. **C86**, 014908 (2012).
[30] H. J. Drescher and Y. Nara, Phys. Rev. **C75**, 034905 (2007).
[31] H.-J. Drescher and Y. Nara, Phys. Rev. **C76**, 041903 (2007).
[32] Y. Mehtar-Tani and G. Wolschin, Phys. Rev. Lett. **102**, 182301 (2009).
[33] Y. Mehtar-Tani and G. Wolschin, Phys. Rev. **C80**, 054905 (2009).

[34] A. Bazavov *et al.* (HotQCD), Phys. Rev. **D90**, 094503 (2014).

[35] A. Bazavov *et al.* (HotQCD), Phys. Rev. **D86**, 034509 (2012).

[36] H. T. Ding, S. Mukherjee, H. Ohno, P. Petreczky, and H. P. Schadler, Phys. Rev. **D92**, 074043 (2015).

[37] A. Monnai and B. Schenke, Phys. Lett. **B752**, 317 (2016).

[38] G. Denicol, A. Monnai, and B. Schenke, Phys. Rev. Lett. **116**, 212301 (2016).

[39] A. Buchel, Phys. Lett. **B663**, 286 (2008).

[40] M. Natsuume and T. Okamura, Phys. Rev. **D77**, 066014 (2008), [Erratum: Phys. Rev.D78,089902(2008)].

[41] B. Berdnikov and K. Rajagopal, Phys. Rev. **D61**, 105017 (2000).

[42] S. Mukherjee, R. Venugopalan, and Y. Yin, Phys. Rev. **C92**, 034912 (2015).

[43] A. Monnai and T. Hirano, Phys. Rev. **C80**, 054906 (2009); Nucl. Phys. **A847**, 283 (2010).

[44] S. Mukherjee, R. Venugopalan, and Y. Yin, Phys. Rev. Lett. **117**, 222301 (2016).

[45] F. Karsch, D. Kharzeev, and K. Tuchin, Phys. Lett. **B663**, 217 (2008).

[46] L. Adamczyk *et al.* (STAR), Phys. Rev. Lett. **112**, 162301 (2014).

[47] L. Adamczyk *et al.* (STAR), Phys. Rev. Lett. **116**, 112302 (2016).

[48] H. Song and U. W. Heinz, Phys. Rev. **C81**, 024905 (2010); J. Noronha-Hostler, G. S. Denicol, J. Noronha, R. P. G. Andrade, and F. Grassi, Phys. Rev. **C88**, 044916 (2013); J. Noronha-Hostler, J. Noronha, and F. Grassi, Phys. Rev. **C90**, 034907 (2014); S. Ryu, J. F. Paquet, C. Shen, G. S. Denicol, B. Schenke, S. Jeon, and C. Gale, Phys. Rev. Lett. **115**, 132301 (2015).

[49] G. Torrieri, B. Tomasik, and I. Mishustin, Phys. Rev. **C77**, 034903 (2008); G. Torrieri and I. Mishustin, Phys. Rev. **C78**, 021901 (2008); K. Rajagopal and N. Tripuraneni, JHEP **03**, 018 (2010); M. Habich and P. Romatschke, JHEP **12**, 054 (2014).

[50] P. Schofield, J. D. Litster, and J. T. Ho, Phys. Rev. Lett. **23**, 1098 (1969).

[51] J. Zinn-Justin, Phys. Rept. **344**, 159 (2001).

[52] M. Stephanov, Phys. Rev. Lett. **107**, 052301 (2011).

Appendix A: Parametrization of correlation in Ising variables

For completeness, in this section, we explain the parameterization of the critical correlation length $\xi(r,h)$ in the critical regime in terms of the Ising variables r and h used in this paper. For this purpose, we only need to know the equilibrium magnetization $M(r,h)$ as ξ can be computed by taking derivatives of $M(r,h)$ with respect to h at fixed r,

$$\xi^2 = \frac{1}{H_0}\left(\frac{\partial M(r,h)}{\partial h}\right)_r . \tag{A1}$$

Here H_0 is a dimensionful parameter (of mass dimension 3) which relates reduced magnetic field h to the unreduced magnetic field. As explained earlier (c.f. footnote 1), we will take critical exponent $\eta = 0$. Therefore R.H.S of (A1), which is nothing but magnetic susceptibility χ_M in Ising model, is proportional to ξ^2. This relation have been widely used in the previous studies (see for example Ref. [12]).

To parametrize $M^{\rm eq}(r,h)$, we use the linear parametric model [50, 51]. In this parametrization, one introduces two new variables R,θ which are related to (dimensionless) Ising variable r,h as

$$r(R,\theta) = R(1-\theta^2)\,, \qquad h(R,\theta) = \Delta h\, R^{\beta\delta}\, \tilde{h}(\theta)\,, \tag{A2}$$

Following Ref. [52], we will use

$$\tilde{h}(\theta) = 3\theta\left[1 - \left(\frac{(\delta-1)(1-2\beta)}{(\delta-3)}\right)\theta^2\right] . \tag{A3}$$

Here β,δ are standard critical exponents and we will use the values obtained from mean field theory, $\beta = 1/3, \delta = 5$. In these R,θ variables, $\theta = 0$ corresponds to the crossover line and $|\theta| = \sqrt{3/2}$ corresponds to the coexistence (first order transition) line. The equilibrium "magnetization" $M_0^{\rm eq}(r,h)$(or σ_0) is given by

$$M^{\rm eq}(R,\theta) = M_0 R^\beta \theta\,, \tag{A4}$$

where M_0 sets the scale of "magnetization". The parametrization introduced describes the equation of state with a precision sufficient for our purpose.

We now compute $\kappa_n^{\rm eq}$ using Eq. (A1) and Eq. (A4). Explicitly, we have

$$\xi^2 = \frac{M_0}{H_0}\frac{1}{R^{4/3}(3+2\theta^2)} . \tag{A5}$$

One could then determine $\xi(r,h)$ consequently from (A5) using (A2).

Notice: This manuscript has been co-authored by employees of Brookhaven Science Associates, LLC under Contract No. DE-SC0012704 with the U.S. Department of Energy. The publisher by accepting the manuscript for publication acknowledges that the United States Government retains a non-exclusive, paid-up, irrevocable, worldwide license to publish or reproduce the published form of this manuscript, or allow others to do so, for United States Government purposes. This preprint is intended for publication in a journal or proceedings. Since changes may be made before publication, it may not be cited or reproduced without the authors permission.

DISCLAIMER: This report was prepared as an account of work sponsored by an agency of the United States Government. Neither the United States Government nor any agency thereof, nor any of their employees, nor any of their contractors, subcontractors, or their employees, makes any warranty, express or implied, or assumes any legal liability or responsibility for the accuracy, completeness, or any third partys use or the results of such use of any information, apparatus, product, or process disclosed, or represents that its use would not infringe privately owned rights. Reference herein to any specific commercial product, process, or service by trade name, trademark, manufacturer, or otherwise, does not necessarily constitute or imply its endorsement, recommendation, or favoring by the United States Government or any agency thereof or its contractors or subcontractors. The views and opinions of authors expressed herein do not necessarily state or reflect those of the United States Government or any agency thereof.